

**Biophysical Journal, Volume 112**

**Supplemental Information**

**Cell Division Induces and Switches Coherent Angular Motion within  
Bounded Cellular Collectives**

**Michael J. Siedlik, Sriram Manivannan, Ioannis G. Kevrekidis, and Celeste M. Nelson**

## Supplementary Figure and Movie Legends

**Figure S1: The framework of simulated CAM.** The minimalistic model of cell migration within a bounded tissue is based upon a force balance that takes into account near-range (a) cell-cell repulsion, (b) flocking interactions, (c) persistence, and random fluctuations. (d) Additionally, neighboring cells are weakly attracted towards mitotic cells. (e) Cell division is specified to occur consistently with experimentally observed doubling times, distribution of division angles, and distances between daughter cells. See Figure S3. (f) A snapshot from simulations in which the green cell divides to produce two daughter cells.

**Figure S2: Cells exhibit persistent motion in the experiments.** This histogram shows the change in angle between successive trajectories of each experimentally tracked cell, in which cells exhibit a tendency to continue moving in a similar direction. \* $p < 0.05$ , chi-square goodness of fit test comparing data to a uniform distribution.

**Figure S3: Simulated cell divisions are based upon multiple experimentally observed details.** It is observed in the experiments that (a) a given cell tends to exhibit a cell cycle duration of  $13.3 \pm 1.7$  hrs, (b) daughter cells emerge separated by approximately  $15 \mu\text{m}$ , and (c) the orientation of cell division is biased towards occurring perpendicular to the radial axis.

**Figure S4: Simulated cells are specified to preferentially divide perpendicular to the radial axis.** The distribution of simulated division angles closely resembles that from the experiments. See Figure S3c.

**Figure S5: The attraction term in the simulations accounts for experimentally-observed motion of non-mitotic cells towards nearby dividing cells.** (a) We incorporate an attraction term into the simulations to account for changes in motion of non-mitotic cells as nearby mitotic cells round up and eventually divide. (b) In the experiments, non-mitotic cells within 20  $\mu\text{m}$  of a mitotic cell preferentially move towards that cell immediately before it undergoes cytokinesis.

**Figure S6: Suppressing mitosis does not affect individual cell speed.** Histograms of the distances moved by cells within (a) untreated and (b) mitomycin-C-treated tissues.

**Figure S7: Blocking cell division with aphidicolin reduces CAM.** (a) Treatment with aphidicolin abolishes cell divisions over a 14-hour period of observation. (b) The fraction of tissues exhibiting at least one period of CAM is reduced in tissues treated with aphidicolin, as compared to untreated tissues. (c) The fraction of rotating tissues that exhibit switches in the direction of CAM is reduced in tissues treated with aphidicolin, compared to untreated tissues. To generate these plots, rotational motion starting 90 minutes after the beginning of experimental observation was analyzed to ensure that cell division did not immediately precede the period of analysis. \* $p < 0.05$ .

**Figure S8: The location of a cell division is important in tissues of various sizes.** Square tissues with edge lengths of 40  $\mu\text{m}$  (N = 20 tissues), 50  $\mu\text{m}$  (N = 18 tissues), and 90  $\mu\text{m}$  (N = 22 tissues) were observed with timelapse microscopy. In all cases, a significantly higher fraction of

cell divisions promoted CAM (see Methods) at the periphery of the tissue compared to the interior of the tissue. \* $p < 0.05$ .

**Movie S1: Timelapse imaging of engineered monolayers consisting of mammary epithelial cells reveal that these tissues exhibit dynamic CAM.**

**Movie S2: Untreated tissues exhibit dynamic CAM.**

**Movie S3: Tissues treated with mitomycin C exhibit reduced CAM.**

**Movie S4: Simulated tissues that include cell divisions show dynamic CAM.**

**Movie S5: Simulated tissues that do not allow for cell divisions do not exhibit dynamic CAM.**

Figure S1

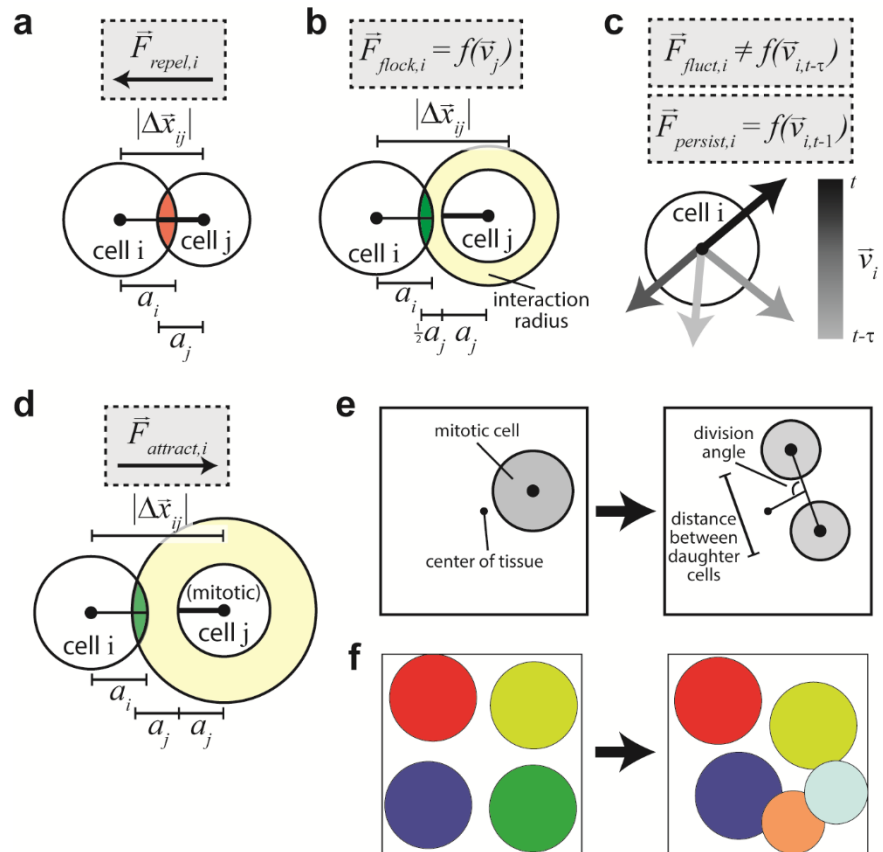


**Figure S2**

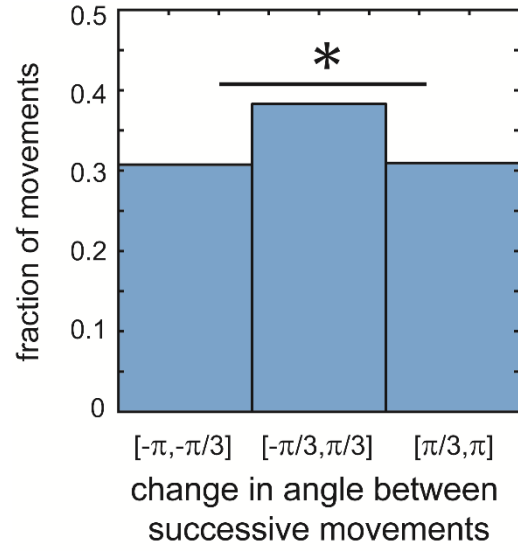


**Figure S3**

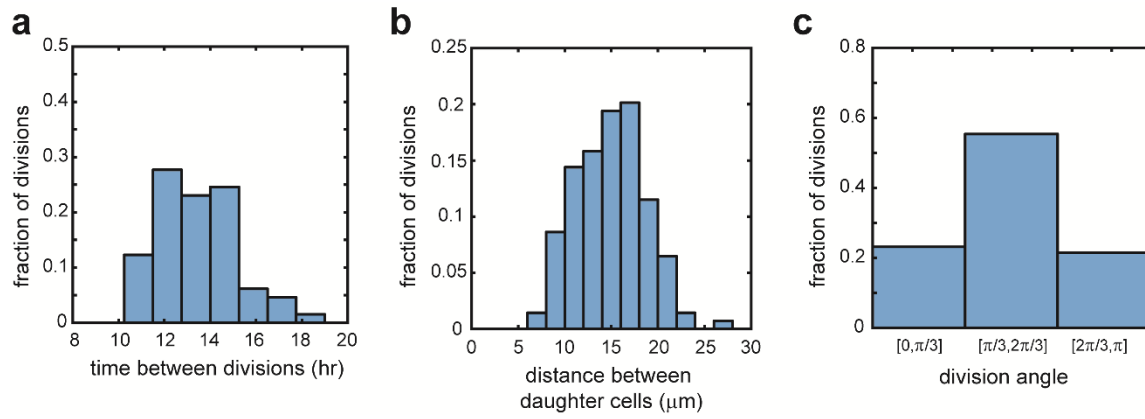


**Figure S4**

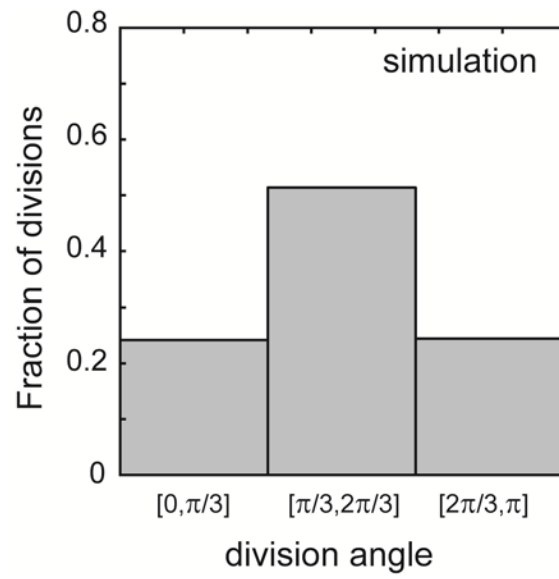
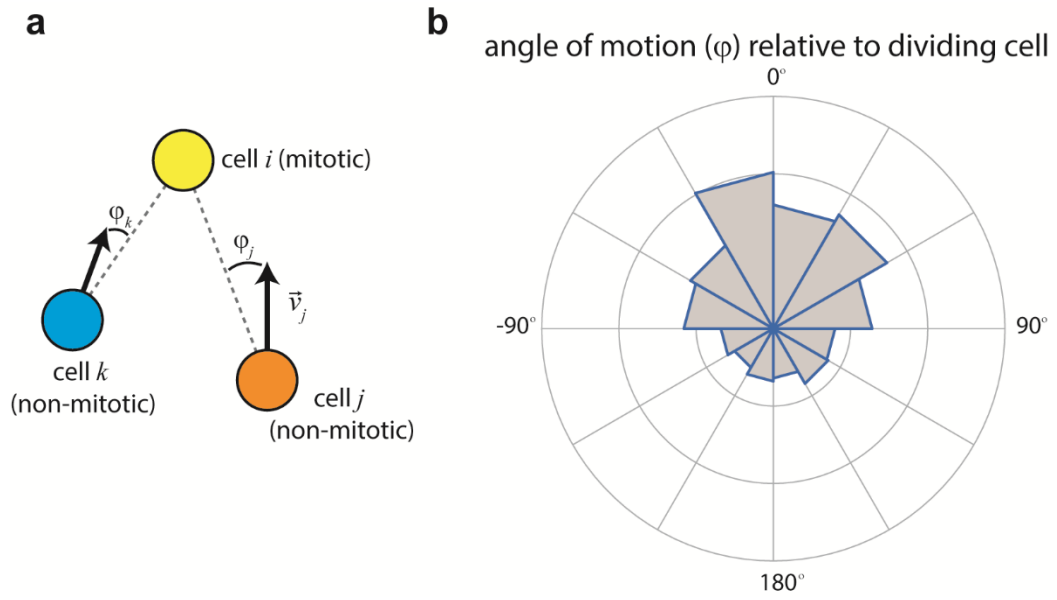
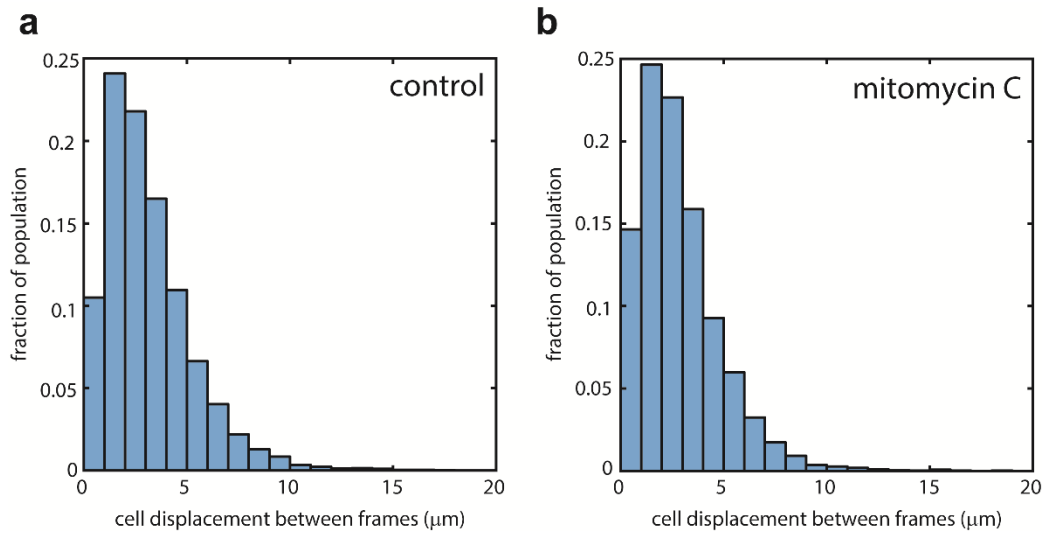




Figure S5



**Figure S6**



**Figure S7**

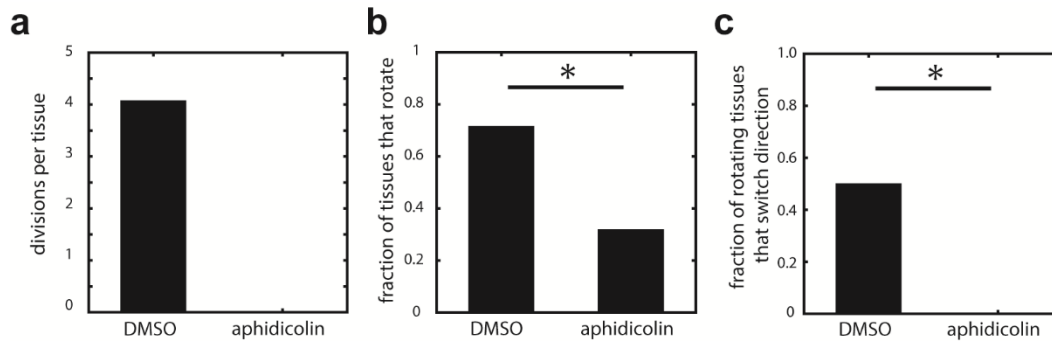


**Figure S8**

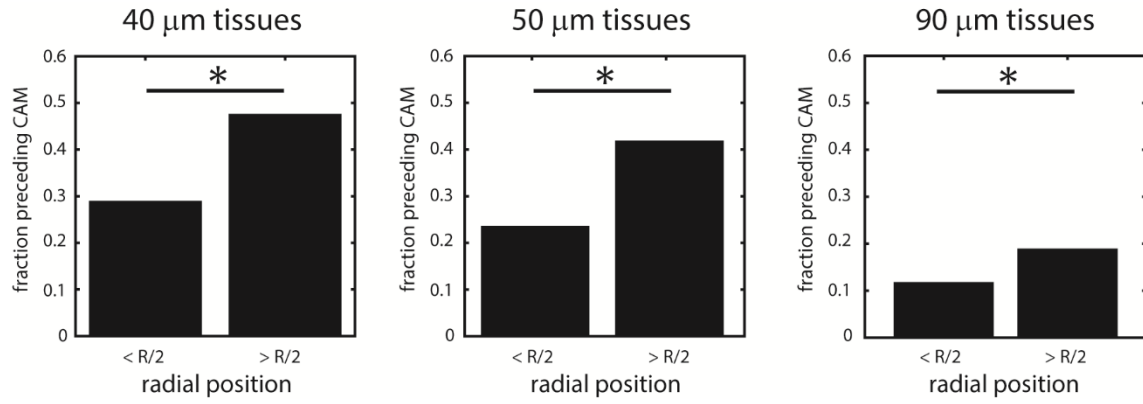


**Table S1: Parameters and terms used in simulations**

Parameter	Description	Estimated relevant values*	Value used*	Ref.
A1	Repulsion constant	3 – 30 $\mu\text{m}$ / (3 min)	6	Ref. 29
A2	Flocking constant	0.3 – 3 $\mu\text{m}$ / (3 min)	0.6	Fig. S5a
A3	Persistence constant	0.03 – 0.3 $\mu\text{m}$ / (3 min)	0.05	Fig. S2
A4	Fluctuation constant	0.3 – 3 $\mu\text{m}$ / (3 min)	0.3	
A5	Attraction constant	3 – 30 $\mu\text{m}$ / (3 min)	3	
$R$	Interaction radius**	Nearest neighbors	$\underline{a_i + \frac{3}{2}a_j}$	Fig. S1
$a$	Cell radius		11	
-	Tissue boundary	50 $\mu\text{m}$	50	
-	Cell doubling time	11.5-15 hr	Randomly selected from [11.5,15]	Fig. S3a
-	Distance between daughter cells	5 – 25 $\mu\text{m}$	15	Fig. S3b
-	Cell division orientation	Preferentially $\pi/2$	See Fig. S4	Fig. S3c

\* The estimated range and values used are reported in 3 minute time increments because simulation positions were updated at time steps corresponding to 3 experimental minutes.

\*\* The interaction radius was specified to allow for interactions between cells in the immediate vicinity of one another and so the interaction radius was chosen to allow for cell  $j$  to interact with cell  $i$  if the distance between the outer boundaries of each cell was less than  $\frac{1}{2}a_j$ . This is equivalent to the distance between the center points of each cell being less than  $a_i + \frac{3}{2}a_j$ .